

## Three-Dimensional Turbomachinery Inverse Blade Design: An Application to Axial Flow Compressor

Wanchai Asvapoositkul<sup>1</sup> and Thanongsak Amphonkiat

King Mongkut's University of Technology Thonburi

Suksawat 48 Rd., Bangkok 10140

Tel: +662-4709123 Fax: +662-4709111 E-mail: wanchai.asv@kmutt.ac.th<sup>1</sup>

### Abstract

The computational method based on three-dimensional inverse design in inviscid flow is applied to the design of 0.78 m diameter single stage axial flow compressor. By applying this method, the blade shape is computed for a specified distribution of swirl distribution. A useful design of the method is that the blade shape is compatible with prescribe the surface velocity. Therefore, an improvement in the performance is expected. The experimental data showed that the design blade gave excellent agreements from those of the computed results. The flow in the designed compressor rotor closely approximates that of viscous analysis code and shows no breakdown of the flow within the designed blade profile.

### Introduction

The basic ideas of an inverse methodology for the design of 2D turbomachinery blade described by Hawthorn et. Al. [1] and Asvapoositkul [2]. A study of inverse design for turbomachinery blades was discussed in great detail by Dang [3] and applied to radial inflow turbines by Zangeneh [4] and Yang et. al. [5].

The fluid flow in turbomachinery is very complex and usually three-dimensionality. Also, specification and enforcement of proper boundary conditions are essential to accurately capture the physical of the flow. The flow conditions are also related to the blade shape. If they are not matched, high loss may be expected. The main difficulty is that a change of blade shape at any location affects the flow at other parts of the blade. In inverse design method, the blade surfaces are generated according to the given conditions and the boundary conditions. This is achieved by the iterative manner from the blade boundary condition. When the solution converges, the blade shape is adjusted so that the flow is everywhere tangent to the blade surface and the blade produces the prescribed pressure loading.

The method presented is based on the method of solving by Amphonkiat and Asvapoositkul [6].

Application of this theory to the design of a single stage axial flow compressor is reported. The flow is three-dimensional, incompressible and inviscid. The blades are assumed to have zero thickness and zero incidence so that there are no stagnation point at the leading edges.

### Design method

Blade geometry is generated after geometrical parameters such as hub-tip ratio, number of blades, blade axial width, and rotational speed have been chosen, as well as the overall deflection, the schedule of pitchwise averaged tangential velocity,  $\bar{V}_\theta$  is prescribed at all points within the blades row. Rotor is designed to have the vorticity dependence on the axial distribution only or free-vortex swirl schedule of the form  $r\bar{V}_\theta = \bar{r}\bar{V}_\theta(z)$  with no trailing vorticity. This condition is imposed across the blade surface.

### Rotor Impeller Design

The impeller's design operating condition was as follows:

Rotational speed = 850 rpm

Mass flow = 12.54 kg/s

Tip diameter = 0.78 m

Hub diameter = 0.45 m

Number of blades = 17

The specified distribution of  $r\bar{V}_\theta$ , non-dimensionalised by the blade tip speed and tip radius, is shown in Fig. 1. At the leading and trailing edges, the derivative of  $r\bar{V}_\theta$  in the axial direction were set to zero to satisfy the no-incidence and Kutta-Joukowski conditions, respectively. The design of the present inverse

method is based on the condition that the flow velocity vectors tangential to the blade surface. This flow is divided into circumferentially average and periodic terms. Therefore the blade shape according to this condition is defined as [6]:

$$\left(\bar{v}_z + \hat{v}_z\right) \frac{\partial f}{\partial z} + \left(\bar{v}_r + \hat{v}_r\right) \frac{\partial f}{\partial r} = \frac{r \bar{v}_\theta}{r^2} + \frac{\hat{v}_\theta}{r} - \omega \quad (1)$$

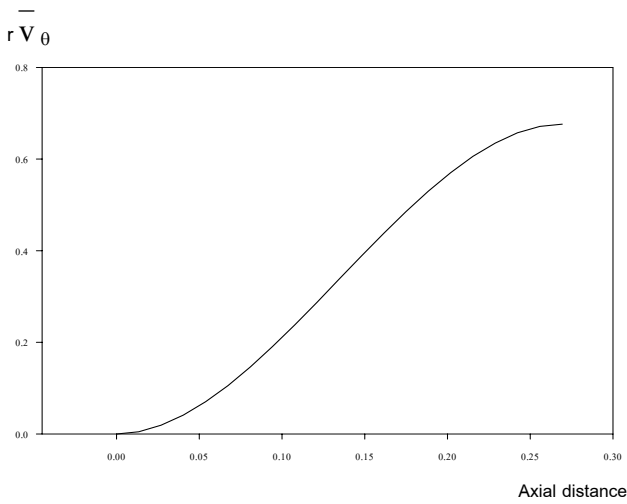


Fig 1 Specified  $r \bar{v}_\theta$  distribution

In this equation  $f$  is the wrap angle,  $z$  denotes the axial distance, the circumferentially average velocities are denoted with superscript  $\bar{\cdot}$ , the periodic velocities are denoted with superscript  $\hat{\cdot}$  and  $\omega$  is angular velocity. To solve for an initial blade profile, all the periodic terms are neglected to in equation (1). Then, the following iterative scheme is used to update the blade profile:

1. The circumferentially average terms are computed by

solving equation (2) for the Stokes stream function  $\psi$

$$\frac{\partial^2 \psi}{\partial r^2} - \frac{1}{r} \frac{\partial \psi}{\partial r} + \frac{\partial^2 \psi}{\partial z^2} = -r \left[ \frac{\partial r \bar{v}_\theta}{\partial r} \frac{\partial f}{\partial z} - \frac{\partial r \bar{v}_\theta}{\partial z} \frac{\partial f}{\partial r} \right] \quad (2)$$

where  $\bar{v}_r = -\frac{1}{r} \frac{\partial \psi}{\partial z}$  and  $\bar{v}_z = \frac{\partial \psi}{\partial r}$

2. The periodic terms are computed by solving equation (3)

for the potential function  $\phi$

$$\frac{\partial^2 \phi_n}{\partial r^2} + \frac{1}{r} \frac{\partial \phi_n}{\partial r} + \frac{\partial^2 \phi_n}{\partial z^2} - \frac{n^2 B^2}{r^2} \phi_n = \frac{2e^{-inBf}}{inB} \left[ \nabla^2 r \bar{v}_\theta \right] - 2e^{inBf} \left[ \frac{\partial r \bar{v}_\theta}{\partial r} \frac{\partial f}{\partial r} + \frac{\partial r \bar{v}_\theta}{\partial z} \frac{\partial f}{\partial z} \right] \quad (3)$$

where  $\hat{v} = \nabla \phi(r, \theta, z) - S(\alpha) \nabla r \bar{v}_\theta$ ,  $B$  = the number of the blades,  $i$  = imaginary number  $\sqrt{-1}$ ,  $n$  = integer,  $S$  = periodic saw tooth function

3. The blade wrap angle  $f$  is updated by solving equation (1).

The sequence represents one cycle of an iteration procedure and performs until the convergence of  $f$  is reached. The blade wrap angle from the given design conditions at various spanwise locations are shown in Fig. 2. The shape is characterized by a steep gradient near the blade leading edge and corresponds to loading distribution that satisfies the Kutta condition and zero incidence. The blade profiles and geometry (with thickness) are shown in Fig. 3.

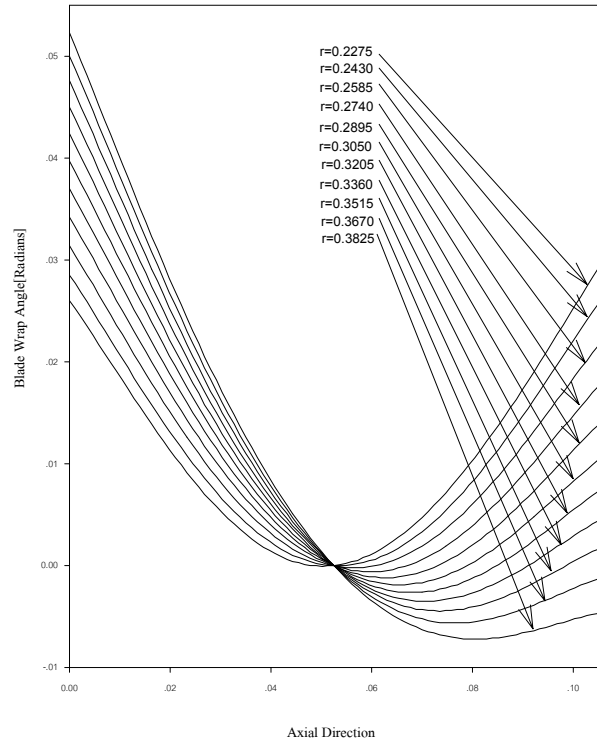


Fig. 2 Blade profile of 3-D axial flow compressor

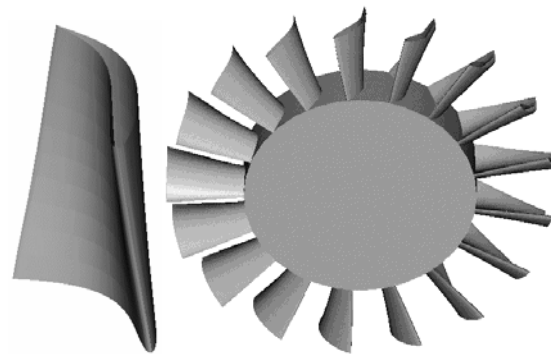


Fig 3 Blade geometry

### Comparison with Analysis Program and Experimental results

In order to check the accuracy of the design method, the flow through the compressor designed by this method was analyzed by using 3D viscous flow analysis program (Navier-Stokes

equations). The grid used for the analysis consisted of 17 spanwise, 17 azimuthal and 67 streamwise (17 upstream, 33 at the blade and 17 downstream). In order to capture the viscous layers, a fine mesh near the wall is required. Therefore, the nearest grid point along the wall was set  $y^+ = 1$ . In this calculation the k- $\epsilon$  model is used to evaluate the turbulent eddy viscosity. The computational mesh is shown in Fig. 4. The convergence of the calculation is speed-up by applying the multigrid technique.

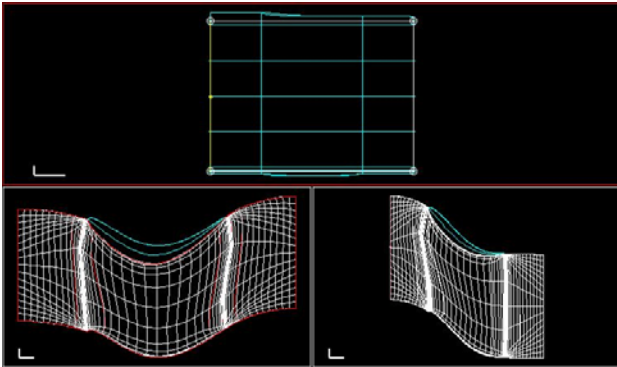


Fig. 4 Blade to blade of the mesh used in the analytical calculation

The blade geometry shown in Fig. 3 was manufactured by a casting process and installed in the test rig as shown in Fig. 5 for testing. The Pitot tube and claw-type yaw meter are used to measure flow velocity at the inlet and the outlet of blade. The claw-type yaw probes having a  $120^\circ$  included angle between the arms. The probe is held by the carriage which can be rotated with  $360^\circ$  and moved from hub to tip.

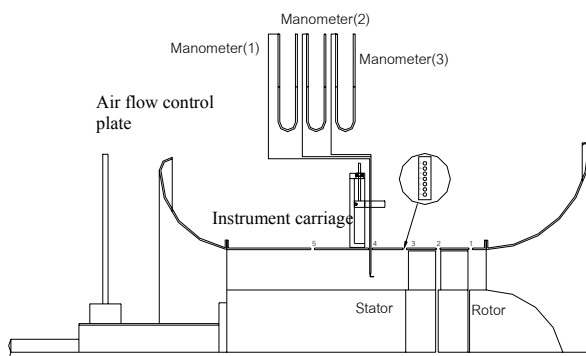


Fig. 5 Schematic drawing of axial flow compressor test installation

## Result

In this investigation, the blade geometry is computed by inverse design method. The blade shape was generated for ensuring that the velocities are delivered and with optimum

aerodynamic performance. A back-check analysis of flow through the designed profile using the analysis program (Navier-Stokes equations). The surface pressure distribution from both methods is shown in Fig. 6. From this we see that the stagnation point is located directly on the profile leading edge, resulting in smooth entry flow as illustrated by Fig. 7. The pressure on the upper convex surface falls to a minimum value of  $c_{p,min} = -1.25$  at about the mid chord and then diffuses steadily towards the exit value of  $-0.6$ . The predicted pressure coefficient from both methods are slightly difference especially on the lower surface. Despite this set back, Fig. 7 gives us a firm indication that we have selected an aerodynamically acceptable blade geometry. Confirm that this blade is designed as intend in Inverse Design. It should be noted that the Inverse design method is based upon potential flow modeling while the analysis program is based upon viscous flow Navier-Stokes equations. The blade thickness is also difference in the two methods since the Inverse Design the blade is assumed to be very thin. The velocity vector at the mid-span from the analytical calculation is shown in Fig. 8 where shows no breakdown of the flow within the designed blade profile.

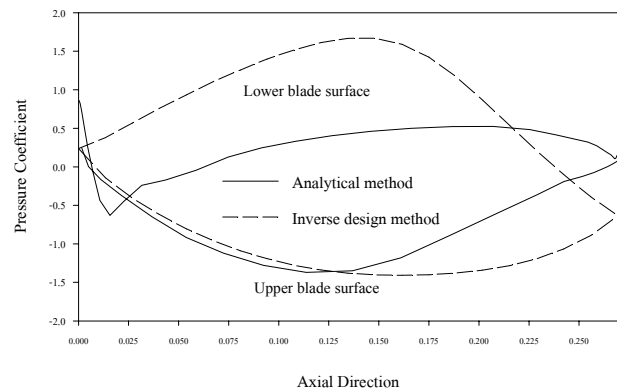


Fig. 6 Pressure distribution at mid-span

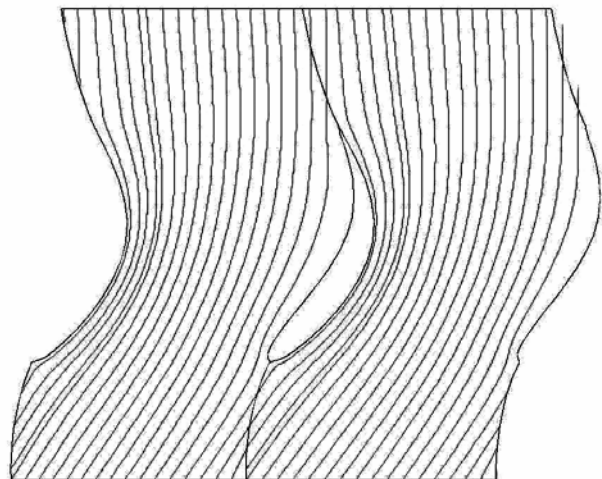


Fig. 7 Stream line at mid-span from analytical calculation

It is helpful to compare the measure velocities with that from the analysis program. Theoretically, there is to be zero swirl at entry, that is  $c_{\theta 1} \approx 0$ . We can see the trend in Fig. 9. The variation of axial velocity along the blade at the inlet and outlet of the rotor are shown in Fig. 11 and Fig. 14, respectively. This illustrates that the velocity is fairly constant over the blade height. As can be seen the solid boundaries of the rotor exert more influence on the velocity profile (no-slip wall conditions). From Fig. 10 and Fig. 11 the entry velocity,  $c$ , is nearly axial. At the downstream of the rotor on the other hand there of course always be some swirl velocity  $c_{\theta 2}$ , see Fig. 12. In general, the results are in the same trend and within acceptable accuracy.

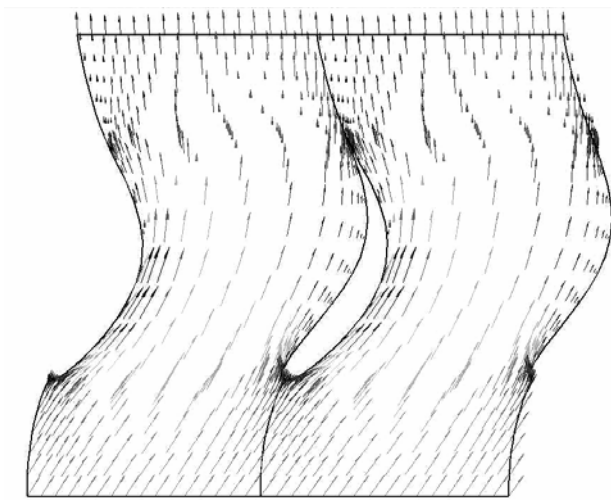


Fig 8 velocity vector at mid-span from analytical calculation

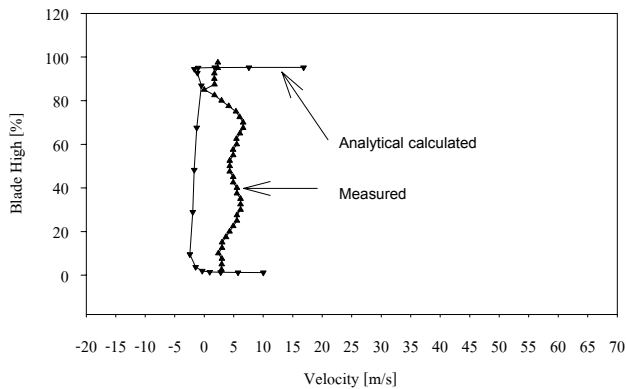


Fig 9 Tangential velocity profile at position 1

**Concluding Remarks**

In this paper the inverse design was extended to deal with the design of the axial compressor. The inverse design method is used to select suitable blade profiles which will perform with stable and low loss flow. The analytical program and the measured velocities were conducted to back-check the result

from the inverse method. We observe the data matched to that design conditions. The pressure loading indicates that at the operating point, rotor is mid-loaded with zero incidence in the inverse mode. A smooth blade pressure loading distribution corresponds to static pressure distribution on the blade surface. The predicted velocities on the other hand are almost and perfectly acceptable.

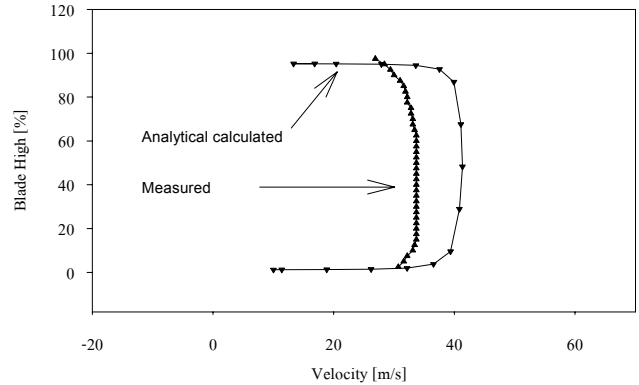


Fig 10 Absolute velocity profile at position 1

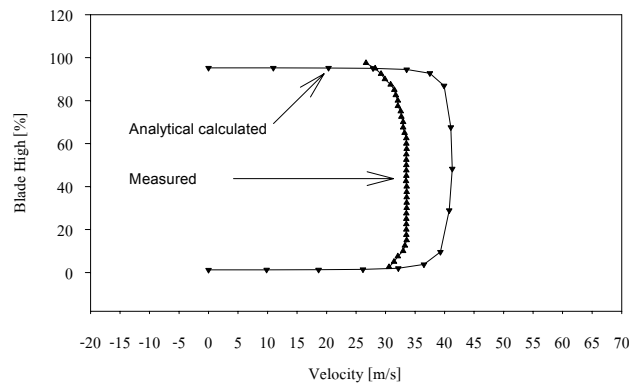


Fig. 11 Axial velocity profile at position 1

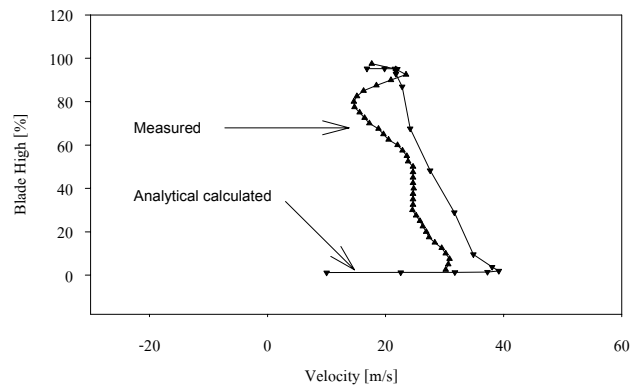


Fig 12 Tangential velocity profile at position 2

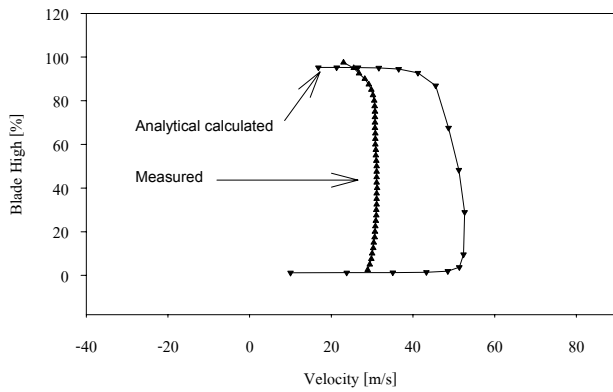


Fig. 13 Absolute velocity at position 2

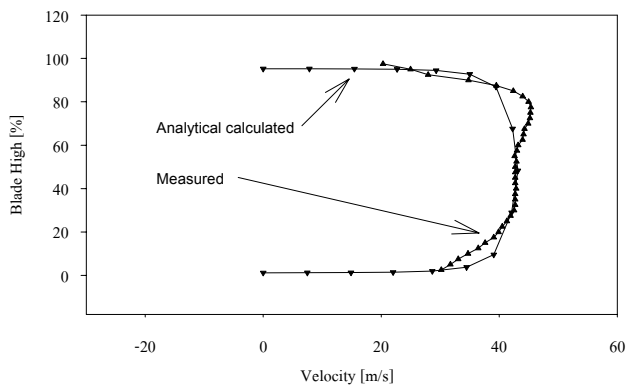


Fig 14 Axial velocity profile at position 2

An Application to Radial Inflow Turbines”, ASME Journal of Turbomachinery Vol. 115, April 1993, pp. 602-613

[6] Amphonkiat, Thanongsak and Asvapoositkul, Wanchai, “Inverse Design Calculation for Turbomachinery Blades (Numerical Method)”, KMUTT Research and Development Journal, Vol. 23, No. 2 May-August 2000

### Acknowledgements

This research was partially supported by National Energy Policy Office of Thailand (NEPO in that time).

### References

- [1] Hawthorne, W.R., Wang, C., Tan, C.S., and McCune, J.E., “Theory of Blade Design for Large Deflections, Part I: Two-Dimensional Cascade”, ASME Journal of Engineering for Gas Turbines and Power, Vol. 106, April 1984, pp. 346-353
- [2] Asvapoositkul, Wanchai, “Computational Method for Inverse Blade Design”, Research and Development Journal of the Engineering Institute of Thailand, Vol. 7, No. 1, 1996, pp.93-103
- [3] Dang, T.Q., “A fully Three-Dimensional Inverse Method for Turbomachinery Blade in Transonic Flows”, ASME Journal of Turbomachinery, Vol. 115, April 1993, pp. 354-361
- [4] Zangeneh, M., “Three Dimensional Design of a High Speed Radial-Inflow Turbine by a Novel Design Method”, ASME paper 90-GT-235
- [5] Yang, Y.L., Tan, C.S., and Hawthorne, W.R., “Aerodynamic Design of Turbomachinery Blading in Three-Dimensional Flow: